Dynamical analysis of survival of Kosterlitz-Thouless pairs due to pinning

Darwin Chang*
Department of Physics, National Tsing-Hua University, Hsinchu, Taiwan, 30043, Republic of China

Baruch Rosenstein†
Electrophysics Department, National Chiao Tong University, Hsinchu, Taiwan, 30043, Republic of China

Ching-Long Wu‡
Department of Physics, National Tsing-Hua University, Hsinchu, Taiwan, 30043, Republic of China
(Received 17 June 1996)

We investigate the process of annihilation between vortices of opposite flux in superconducting thin films in the presence of randomly distributed pinning centers. The number and distribution of pairs of vortex-antivortex that avoid annihilation due to pinning on two pinning centers is estimated analytically and compared with numerical simulations. The situation can be realized, for example, when the system is quenched from high temperature (above or below the Kosterlitz-Thouless temperature) or when the current is reduced abruptly. Qualitatively two different cases can be distinguished. The simpler one is when the pairs are well separated. In this case, the problem under mild assumptions can be solved analytically. When the vortex pairs are not very rare, the situation is much more complicated because a great variety of processes become significant. We isolate the important ones and construct an iterative (real-space renormalization-group) scheme to describe the behavior of the interacting multivortex system. Some dynamical aspects of pinning and vortex motion are discussed. [S0163-1829(97)04402-0]

I. INTRODUCTION

The Berezinskii-Kosterlitz-Thouless (KT) phenomena in superconducting thin films have been studied intensely both theoretically[1–3] and experimentally in low-T_c superconductors[4] as well as in high-T_c materials.[5] The basic object is the bounded KT pairs of a (Pearl's[6]) vortex and another vortex of opposite flux direction (the ''antivortex''). Their unbinding by current in the low-temperature phase creates nonlinear I-V characteristics, while the thermal unbinding causes the KT phase transition. Above the critical temperature T_{KT} of this phase transition, Ohmic flux-flow resistivity with typical KT temperature dependence has been observed. The dc and ac transport experiments however measure effects of KT pairs only indirectly through their statistical, macroscopic effect.

In a remarkable series of experiments, using the Aharonov-Bohm effect of electron beams scanning the magnetic field on the surface of a superconducting film,[7] tomographic pictures of some apparent KT pairs were obtained. One clearly sees a unit of flux leaving the Pb superconducting film and returning back at a distance of about 1 μm. According to the Boltzmann distribution there should be practically no such large KT pairs since the experimental temperature was that of liquid He, which is far below T_{KT} (by a factor of about 2). Moreover, when a small magnetic field was applied the pair was found among many single vortices oriented along the field. The author's interpretation[7] is that the pair survived cooling because the vortex and the antivortex were trapped by two pinning centers and was not allowed to move closer to annihilate. This picture has not been made more quantitative since then. In this note we consider quantitatively the dynamical problem of the survival of the pairs upon cooling to the temperatures in which quenched disorder exists, while thermal creation of additional pairs is practically absent. The disorder will be idealized as random distribution of identical pinning centers, although generalization to other types of pinning including correlated disorder is simple.

Quite independently of the Hitachi group experiments, a high-resolution scanning superconducting quantum interference device (SQUID) microscope (SSM) technique has been developed recently.[8–10] This allows, in principle, direct observation of KT pairs. Indeed, some of the published magnetic-field distributions on the surface of thin Y-Ba-Cu-O films look like KT pairs [see Ref. 8, Fig. 3(a) in which apparently ''black'' and ''white'' regions contain a fluxon and an antifluxon]. These experiments were carried out at (liquid-helium) temperatures which is even smaller compared to the corresponding $T_{\mathrm{KT}}\approx 90$ K. Therefore, the possibility of thermal excitation should be completely excluded. Most likely pinning is the only explanation for the survival of the pairs.

A priori the probability that a pair will survive due to pinning seems rather small. Most of the KT pairs are tightly bound close pairs. In order to be pinned it is not enough to encounter *one* pinning center. If only one member of a pair is pinned the second member will simply approach the same pinning center and the pair will annihilate at the center. It is necessary that a second pinning center will trap the second member of *the same pair*[11] *simultaneously*. It is not obvious how large is the probability that this will happen. We will show that, while only some events were spotted in the Hitachi experiments, which did not attempt to measure how often these events occur, the probability is large enough and is consistent with the above observations. The picture that we

get is that a quenched superconductor film surface has magnetic dipoles of quite constant size. The number of dipoles is very sensitive to the density of the pinning centers and the conditions that determine the density of vortices. It is not strongly dependent on dynamical effects like vortex mobility unless the dynamical system is pushed to extreme situations.

The presentation is organized as follows. First in Secs. II–IV we investigate the pinning of well separated KT pairs after quenching. In this case one can neglect the influence of other pairs on a given pair and, as we show, dynamical (timing) effects are small. In Sec. II, we formulate the problem by defining a surviving distribution function: a probability that a single KT pair initially separated by distance R_i will be pinned when they are at distance R_f. In Sec. III, attraction of a single vortex by a pinning center in the presence of constant external force **F** applied by an antivortex is studied. This is the basic elementary process. We find a simple rule: the vortex pinning cross section σ is zero if $F<F_{\max}$, where $F_{\max}$ is the maximal force exerted by a pinning center, while $\sigma\approx 2a$ (a is the radius of the pinning center) when $F>F_{\max}$. In Sec. IV, we calculate the survival distribution function. This is done analytically in the low pinning density case by reducing the model to one dimensional. The results of numerical simulations for this problem (for any density) are given. We then compute the surviving fraction in the case of quenching from the temperature below T_{KT}.

In Secs. V–VII we address the more complicated case of pinning involving many vortices and pinning centers. If one quenches from a temperature close to or above T_{KT} or considers a case of current flowing in the film,[2,3] one encounters a situation that vortices initially are not obviously separated into closely bound pairs. Instead, there is a constant density of vortices and antivortices. After quenching they start to move and annihilate with each other. Some of them are pinned, depinned... . Unlike the previous problem, the time dependence (dynamics) is important here. We outline in Sec. V an iterative [renormalization-group (RG)] scheme to understand these processes. The RG step requires investigation of another elementary process: motion of a vortex through or near a pinned KT pair which is given in Sec. VI. In Sec. VII, the diagrammatic representation of various processes is proposed. In Sec. VIII numerical simulation results are presented and compared with the model. Finite-size effects are briefly discussed. Section IX contains concluding remarks. The characteristic quenching time (determining the thermal depinning process) is estimated. A nonthermal mechanism to produce a population of vortices, like external current at low temperature, is also briefly discussed. In this case quenching is an abrupt disappearance or reduction of the external current so that it cannot depin the surviving pairs.

II. SURVIVAL DISTRIBUTION FUNCTION FOR PINNING OF KT PAIRS

Assume at some initial time we have some initial distribution of vortex pairs $N_i(R)$. For example, if the KT pairs are generated thermally well below the KT phase-transition point, this is given by a Boltzmann's factor:[1,3,12]

$$N_i(R_i)=\frac{2z}{\zeta^4}\,e^{-\beta q^2\ln R_i/\zeta}, \tag{1}$$

where $\beta=1/kT$. The fugacity of the pair is $z\equiv e^{2\mu}$, where μ is the chemical potential for creating a vortex but not containing the contributions from the vortex interaction. The cutoff scale ζ is close to the coherence length ξ of a superconductor.[3] The chemical potential is related, but not equal to the *core* energy $E_c\approx\pi\xi^2 d(H_c^2/8\pi)$, where d is the width of the film and H_c is the thermodynamic critical field. There are other ''geometrical'' factors reflecting the short-range structure of the vortex.[12] The ''charge'' q is obtained from the asymptotic form of the interaction of Pearl's vortices. The force between a vortex and an antivortex separated by distance R_i is[6]

$$F=\frac{q^2}{R_i} \tag{2}$$

with $q^2=2d\Phi_0^2/(4\pi\lambda^2)^2$ where λ is the penetration depth and $\Phi_0\equiv hc/2e$.

The distribution can be rewritten in terms of the KT transition temperature since approximately $T_{\mathrm{KT}}=q^2/4$ up to small RG corrections of order z (in superconducting films z is small[12]):

$$N_i(R_i)=\frac{2z}{\zeta^4}\left(\frac{R_i}{\zeta}\right)^{-4T_{\mathrm{KT}}/T}. \tag{3}$$

Note that N has dimensions of $1/\mathrm{cm}^4$, but due to translational and rotational symmetries it depends on single quantity $R_i\equiv|\mathbf{R}_i|$ only.

After quenching from T ($<T_{\mathrm{KT}}$) to a very low temperature (taken to be zero throughout the discussion) the vortices inside the pairs start moving towards each other. If T is not very close to T_{KT}, vortex pairs are well separated. In this case the mean separation between the pairs,[1]

$$D^2\approx\frac{\zeta^2}{2\pi z}\left(\frac{2T_{\mathrm{KT}}}{T}-1\right), \tag{4}$$

is larger then the mean dipole size $\approx\zeta(T_{\mathrm{KT}}/T-1)^{-1}$. This means that the dipole ''electric'' field from other KT pairs [which, in two dimensions (2D) falls off as $1/r^2$] is very small and practically does not deflect the particles from the straight line motion towards each other. If not for the pinning centers, the KT pairs would have all annihilated very soon (see an estimate in Sec. IX). But if the pinning density is large enough there exists a possibility that both particles will be pinned at some distance R_f from each other. We call this probability density the survival distribution $P(\mathbf{R}_f,\mathbf{R}_i)$. The final distribution of the surviving pair will be given by

$$N_f(R_f)=\int d\mathbf{R}_i P(\mathbf{R}_f,\mathbf{R}_i)N_i(R_i). \tag{5}$$

Due to rotational symmetry the survival distribution depends only on three out of four variables: the lengths R_i and R_f and the relative angle between them (translational symmetry had already been taken into account in the definition of the function). Before calculating this function we discuss an idealized model of pinning of a vortex in the external homogeneous field. This field is produced by the antivortex companion of the vortex.

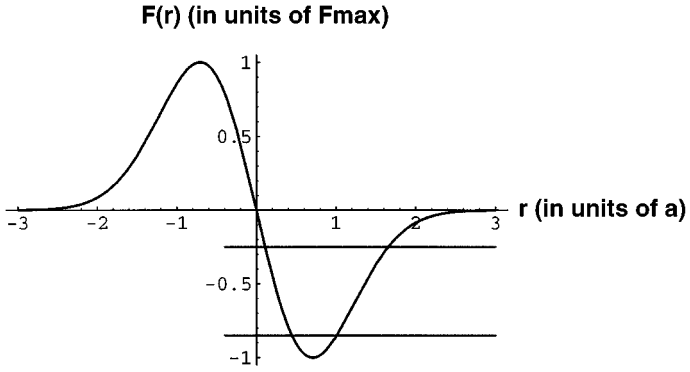

FIG. 1. Attraction of a vortex to ''inverted Gaussian'' type pinning center under influence of force **F**. The two fixed points are intersections of the constant force line with the potential. Cases of small and large force are shown.

III. PINNING OF A VORTEX IN HOMOGENEOUS FIELD

The potentials profiles of ''pointlike'' pinning centers in low and high-T_c superconductors are still not well understood.[13] One estimates these potentials, or forces rather, applied on vortices using various indirect methods: flux flow, magnetic noise due to thermal depinning, creep, . . . ,[9,14] and, in some cases, direct observation of pinning centers. There are several mechanisms of pinning. An important one is simply the advantage that vortices can take by placing the core inside small (compared to relevant core size) regions of a sample in which superconductivity is destroyed. A popular choice of the short-range pinning potential is the ''inverted Gaussian'' one:

$$U(r) = -U_0 e^{-r^2/a^2}. \tag{6}$$

The typical value of the range a is the coherence length ξ, while the minimal energy U_0 is of the order of condensation energy $\pi d\xi^2(H_c^2/8\pi)$. This leads to the maximal force applied around distance a from the center to be of the order $F_{\max} = \pi d\xi(H_c^2/8\pi)$. We investigated several types of short-range potentials and found that, in fact, for most purposes exact shape is not important: just two characteristics are needed: the cross section, giving the effective range of the pinning center and the maximal force.

Suppose on the way towards its companion antivortex a vortex encounters pinning center located at the origin. The force that the antivortex applies on the vortex is given by Eq. (2). First of all, if the maximal force that the pinning center can produce, $F_{\max}$, is smaller then this, pinning is impossible. This determines the minimal distance at which the problem becomes nontrivial:

$$R_{\min} = \left(\frac{q^2}{F_{\max}}\right) = A\xi. \tag{7}$$

Typically the numerical constant A is larger than 1, but should not be very large according to the above estimates. In simulations and numerical estimates we will take $A=5$. We choose it to be oriented in the positive direction along the x axis. The overall force felt by the vortex is therefore

$$\mathbf{F}_{\text{tot}} = -\nabla U(r) + \mathbf{F}. \tag{8}$$

Ignoring the Magnus-like force,[15] the vortex motion is approximately described by[16,3]

$$\frac{d\mathbf{x}}{dt} = \mu \mathbf{F}_{\text{tot}}, \tag{9}$$

where μ is mobility. The mobility is well known from the flux-flow experiment. Of course one might doubt that, on very short distances, this is still valid. However for a simple rough estimate, one can assume that Eq. (9) is correct on all the scales with the same coefficient μ. For $R_{\min} \gg a \sim \xi$, one can approximate the attractive force between the vortex and antivortex by a constant. In that case, it is easy to analyze the set of autonomous differential equations in Eq. (9). The solution has two fixed points (see Fig. 1) $(x_1,0)$ and $(x_2,0)$, $x_1 < x_2$. They are on the x axis, given by solving the equation:

$$\mathbf{F}_{\text{tot}} = 0$$

or, $F = F_{\text{pin}}(r) \equiv -\nabla U(r)$, see Fig. 1 for the inverted Gaussian case.

The first one, x_1, closer to the center, is a stable fixed point, while x_2, close to the edge of the pinning potential, is unstable (Fig. 2). When $F=0$ obviously any vortex will be pinned. In this case $x_1=0$, while $x_2 \to \infty$. At small F the attractor moves a bit from zero, while x_2 very quickly moves to the periphery of the potential. Correspondingly the cross

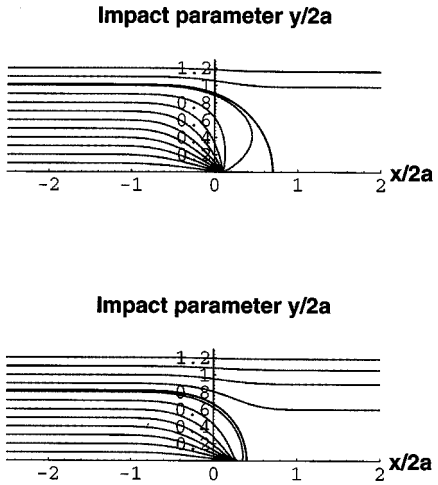

FIG. 2. Pinning on the ''inverted Gaussian'' potential. (a) (the top picture). The case of the small driving force F. The gray lines represent trajectories of the vortex (pinned or escaping the center). The black line is a separatrix. (b) (the bottom picture). The same for the larger driving force.

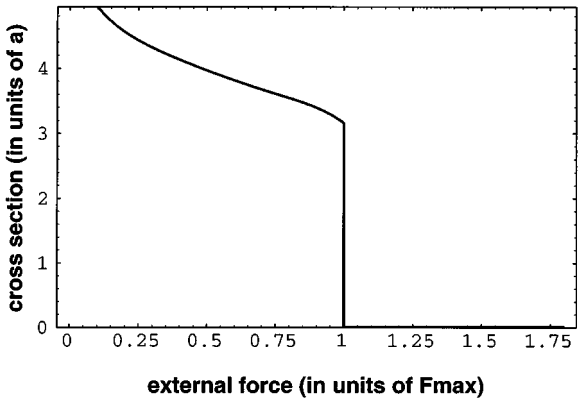

FIG. 3. Pinning cross section σ for the ''inverted Gaussian'' potential as function of the driving force F.

section very quickly stabilizes at about twice the pinning center size, see Fig. 2(a). For F close to the maximal force $F_{\max}$, Fig. 2(b), x_1 approaches x_2 (see Fig. 1) and the cross section grows very slowly. Finally, as F becomes stronger than $F_{\max}$ the pinning center is no longer able to trap the fluxons, σ will abruptly drop to zero, and no fixed point exists, see Fig. 3. The mild divergence at $F=0$ (large separations) is due to the exponential tail of the pinning potential and is insignificant. One can approximate the cross section $\sigma(F)$ for inverse Gaussian potential by a step function

$$\sigma(F)=\sigma\theta(F_{\max}-F), \tag{10}$$

where in the present case $\sigma\approx 4a$. If the potential has a clear cut edge, then σ will resemble a step function even more.

Upon investigating several potentials, we found that for finite ranged potentials, there seems to be a step function behavior for $\sigma(F)$. There is a finite jump just at $F=F_{\max}$. If the pinning force F_{pin} is not strong enough, simply none will get pinned, and $\sigma(r)=0$, this corresponds to the $r<R_{\min}$ case. Nevertheless, once it becomes strong enough to pin something, essentially all the fluxons coming into the range of the potential could not escape. The pinning cross section does not grow slowly from zero but suddenly jumps to a finite value.

One example exhibiting this behavior can be done analytically. For the truncated parabolic potential defined by

$$U(r)=-U_0+\frac{U_0}{a^2}\,r^2 \tag{11}$$

for $r<a$, and zero outside the circle $r=a$, the dynamics is easily solved. It can be shown that the trajectory of the particle inside the circle is just a straight line. Particles are first moving parallel to the external field for $r>a$ and then, once entering the circle, change direction and follow straight lines which intersect the x axis at $x_1=a(F/F_{\max})$, where $F_{\max}=2U_0/a$ is the maximum pinning force at the edge, see Fig. 4. In this case the second fixed point is located at $x_2=-a$ and the cross section is exactly $2a$.

We therefore, as a first approximation, take $\sigma(F)$ to be a step function with certain σ which plays the role of the effective pinning range. This simplifies the calculation of the survival distribution considerably.

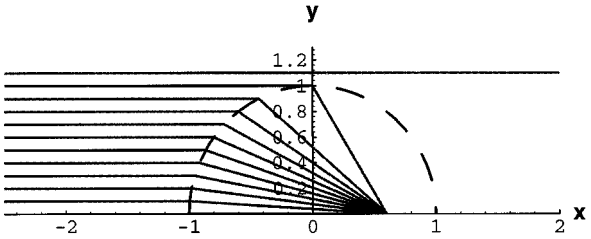

FIG. 4. Attraction to the parabolic potential. Trajectories are straight lines. The direction changes abruptly at the boundary of the pinning center.

IV. REDUCTION TO A ONE-DIMENSIONAL MODEL

Using the step function as the pinning cross section, the problem reduces to one dimensional. Indeed the relative direction of the dipole moment of the shrinking KT pair cannot change much. So

$$P(\mathbf{R}_f,\mathbf{R}_i)=\delta(\theta_i-\theta_f)\,\frac{1}{R_f}\,p(R_f,R_i). \tag{12}$$

Here θ_i and θ_i are polar angles and $p(R_f,R_i)$ is defined to be the one-dimensional survival distribution. Factor $1/R_i$ is introduced to later take into account the Jacobian of the transition to polar coordinates. The one-dimensional density (of dimension $1/\text{cm}^3$) is defined by

$$n(R)\equiv RN(R) \tag{13}$$

with the evolution given by

$$n_f(R_f)=\int_0^\infty dR_i p(R_f,R_i)n_i(R_i). \tag{14}$$

Consider a stripe of width σ. This is the only area where two pinning centers should be located in order to pin the two vortices. The one-dimensional density of pinning centers is

$$\tilde{\rho}\equiv\sigma\rho, \tag{15}$$

where ρ is the 2D density. It is useful to imagine a lattice along the x direction with lattice size b. A one-dimensional lattice is bounded by two vortices at some initial distance R_i. Let $L\equiv R_i/b$ be the number of lattice sites. The probability of having one pinning center on one site is given by $f=b\tilde{\rho}$, with $f\ll 1$, then

$$p(R_f,R_i)=\frac{1}{b}\,f^2(1-f\,)^{(R_i-R_f)/b-2}\left\{\frac{R_i-R_f}{b}+1\right\}\times\theta(R_i-R_f)\,\theta(R_f-R_{\min}) \tag{16}$$

by simple probability counting.

Now one takes the continuum (small b) limit:

$$p(R_f,R_i)=\tilde{\rho}^2e^{-\tilde{\rho}(R_i-R_f)}(R_i-R_f)\,\theta(R_i-R_f)\,\theta(R_f-R_{\min}). \tag{17}$$

This expression is valid for not too high pinning density, so that pinning centers do not overlap with each other. Also its precision is limited by the step-function approximation for the pinning cross section. In practice distance between strong pinning centers is much larger then the center's size ζ. De-

spite this the pinning density can be not very small, in particular if the film is not very thin and short vortex line still can be pinned by few pinning centers.

Now assume that the initial pair distribution is given by the Kosterlitz-Thouless formula Eq. (1). The final distribution is

$$N_f(R_f)=\frac{2z}{\zeta^3 R_f}(\zeta\tilde{\rho})^{4T_{\rm KT}/T-1}e^{\tilde{\rho}R_f}\{\Gamma(3-4T_{\rm KT}/T,\tilde{\rho}R_f) - \tilde{\rho}R_f\Gamma(2-4T_{\rm KT}/T,\tilde{\rho}R_f)\}\theta(R_f-R_{\rm min}). \quad (18)$$

where Γ is an incomplete gamma function. For very large R_f compared to $R_{\rm pin}$ one can show that the asymptotics of $N_f(R_f)$ resembles the initial distribution since these pairs have actually a very large probability to be pinned. There are however very few such pairs to begin with under the conditions of applicability of the Kosterlitz-Thouless distribution formula. Smaller pairs which are very numerous disappear very efficiently and quickly.

Let us estimate the number of surviving pairs larger than a certain size R_0. The size of the KT pairs directly observed in Tonomura's experiment[7] is $R_0\approx 1$ μm. One can take $\zeta\sim\xi\sim 700$ Å, $\sigma\sim 2\xi$, $R_{\rm min}\sim 5\sigma$, $\rho\sim 100(1/\mu{\rm m}^2)$,[9] $z\sim 0.1$. We integrate the $N_f(R_f)$ to get the density for surviving pairs which are larger than $R_0=1$ μm and found ~ 0.1 (pairs/$\mu{\rm m}^2$) for initial $T=T_{\rm KT}$ and 0.001 (pairs/$\mu{\rm m}^2$) for $T=0.75\ T_{\rm KT}$, which corresponds to the average distance between pairs 3.6 and 9.1 μm, respectively. Note that the logarithmic interaction of vortices should be replaced by exponentially weakening one beyond distances of order $\lambda^{\rm eff}$. This increases the probability of pinning, but not significantly in the present case.

The minimal size R_0 should be taken to be the resolution of the scanning SQUID microscope (SSM),[8,10] say $R_0\approx 1$ μm. Smaller loops produce very small magnetic fluxes above the sample and cannot be detected that way. For a Y-Ba-Cu-O thin film with thickness ~ 3000 Å, one can take $\zeta\sim\xi\sim 30$ Å, $\sigma\sim 2\xi$, $R_{\rm min}\sim 5\sigma$, $\rho\sim 600$ $(1/\mu{\rm m}^2)$,[9] $z\sim 0.1$. Assuming that quenching started from $T=T_{\rm KT}/2\sim 40$ K, one gets a very small probability for such large loops according to the above formulas. However in this sample the density may be too high for this simple formula to be correct and in addition some samples like in Ref. 8 are very small (hundreds μm) which leads to large finite-size effects. Starting from the next section we discuss the dense vortex plasma relaxation. We also briefly comment on the finite-size effects in Sec. VIII.

V. QUENCHING OF VORTEX-ANTIVORTEX PLASMA

In previous sections we discussed the relatively simple case when the system of vortices separates into well defined vortex-antivortex pairs. At temperatures significantly below the KT phase-transition temperature, $T_{\rm KT}$, this is indeed the case since pairs are not dense. However very close to $T_{\rm KT}$, the pairs become dense and this assumption breaks down. Above the transition, free vortices appear and one has a plasma rather then a gas of vortex pairs. Even far below KT temperature, if the current is present, it will unbind the pairs, creating a situation which might be better described as weakly correlated plasma. The density of vortices and antivortices in these situations are typically much higher than in the previous case. This by no means leads to a larger number of survivors, as we will see.

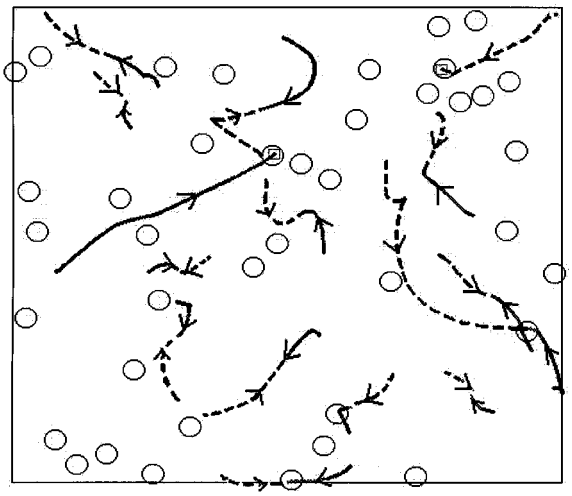

FIG. 5. Typical event in simulation. Gray circles are pinning centers. Solid lines are trajectories of vortices, while the dashed ones are trajectories of antivortices.

Quenching from plasma qualitatively proceeds as follows. At the initial stage the density of vortices is high and interaction between vortices separated by relatively large distances is very effectively screened. At this stage particles which have very close neighbors separated by distance smaller than $R_{\rm min}$ of opposite charge approach each other and annihilate. For more distant pairs, unlike the case of the dilute gas of vortex pairs considered earlier, the choice is not obvious and some spend time ''choosing'' between a few options. Also other particles continuously influence the trajectory which is now not a straight line. At this time most of these relatively close pairs annihilate, but few get pinned. At present circumstances this still does not ensure their survival since (a) they can annihilate with remaining vortices of the opposite charge or, (b) they can be depinned by remaining free vortices of the same charge later.

After the first generation of fluxons annihilated or got pinned, more distant vortices undergo ''pairing.'' They again most likely annihilate with each other, but occasionally could get pinned. They now move in an environment which contains not only empty pinning centers, but also centers with pinned particles of the previous generation. Then again, after this generation are pinned or annihilated, yet more distant vortices pin or annihilate. If one takes the approximation that while one generation is in motion, the vortices of later generations are fixed in position, this can be thought of as an iterative process. This is reasonable as long as the time scale of each generation gets higher than the previous one. We see that, unlike the previous case, timing becomes important. One of the events of this sort is shown in Fig. 5.

Now, in addition to the basic process of a vortex moving towards antivortex and encountering a pinning center, there appears the second elementary process: the vortex encountering a previously pinned KT pair. Such pairs can be easily destroyed. In the next section we study these processes and then propose a quantitative way to describe the evolution of the system.

When a vortex passes close to a pinned pair multitudes of

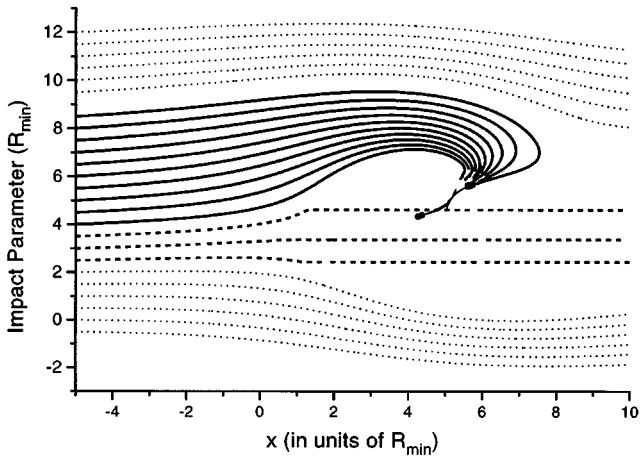

FIG. 6. Motion of a vortex under the influence of both a constant force and the force of a dipole. Solid lines correspond to the σ_1 scattering, in which the incoming vortex annihilates with the pinned antivortex, while its companion remains pinned. Dashed lines denote trajectories of the σ_2 scattering events in which the incoming fluxon kicks the pinned fluxon, depins it causing annihilation. The fluxon itself though continues to move towards its companion. Dotted lines correspond to trajectories for which scattering did not cause any effect: trajectory just bended a little bit.

possibilities exist. They are listed in order of decreasing importance. For definiteness our vortex will be ''positive.''

(i) The vortex annihilates with pinned antivortex, while the other pinned vortex remains pinned (see trajectories denoted by solid lines in Fig. 6).

(ii) The vortex passes by triggering the recombination of the pinned pair (trajectories marked by dashed lines in Fig. 6).

(iii) It causes recombination and itself gets pinned (this is not a frequent event).

(iv) It annihilates with the antivortex, while another vortex gets depinned (this is also very rare).

As far as the net result is concerned (i) and (iii) are equivalent: one pinned vortex left. Processes (ii) and (iv) are also equivalent (one free vortex), so we have to find two cross sections. One can define a cross section, σ_1, which describes events in which the recombination happened, and another cross section σ_2 to describe events in which not only annihilation happened, but, in addition, the remaining particle escaped pinning.

Before we present the result of the simulation in the next section, let us now qualitatively discuss interaction with a dipole. It becomes significant in the area in which the dipole field is comparable with external force F. The dipole field applies a force of order $q^2\lambda/\sigma_d^2$, where λ is the distance between the pinned vortex and antivortex and σ_d is the effective range of their dipole field. The ''external'' force is q^2/R. Therefore $\sigma_d=\sqrt{R\lambda}$. The cross section for the processes in (iii) and (iv) are apparently small because their cross section is of the order $R_{\min}<\lambda\ll R$.

VI. SECOND ELEMENTARY PROCESS: VORTEX PASSES A PINNED PAIR

The method we use to study interaction of a vortex with a pinned pair is very similar to one used in Sec. III. We follow

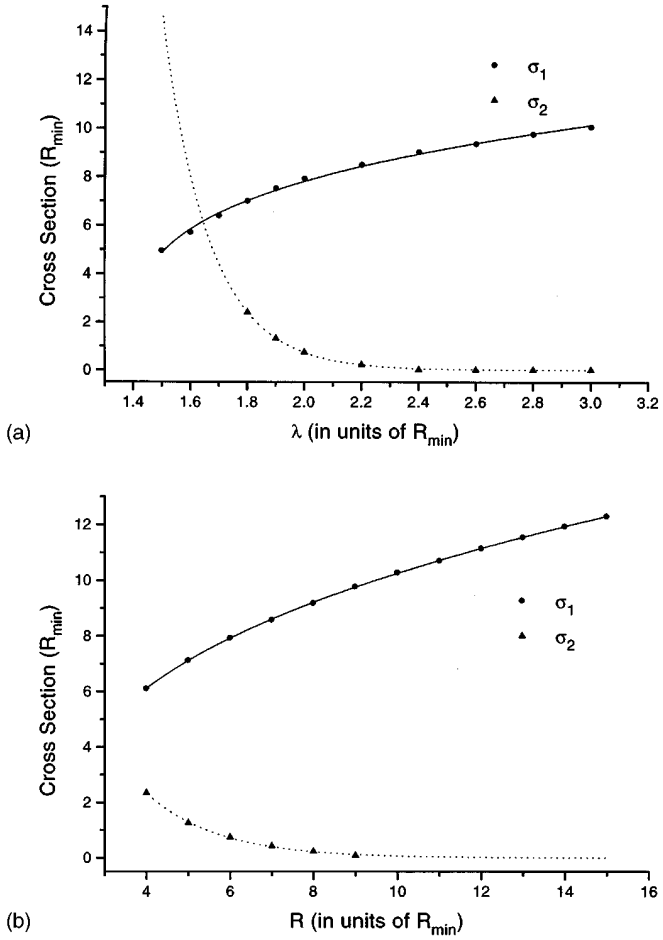

FIG. 7. (a) Cross section of a vortex scattering of a pinned KT pair as a function of dipole size λ. Solid line is σ_1, the vortex ends up pinned, while the dashed line is σ_2, in which case it continues to move towards its companion antivortex. (b) Cross sections σ_1 and σ_2 as functions of the external force $F=q^2/R$ for $\lambda=2R_{\min}$.

trajectories of the vortices under the influence of external force F applied by the second member of the KT pair at a relatively large distance R away. We wish to investigate the dynamics of the vortex and the dipole occupying two pinning centers and interactions between the three participating vortices. A typical event is shown in Fig. 6.

It turns out that although the angle that the dipole moment makes with the direction of motion is important (σ_1 is larger when the pinned antivortex is closer to the incoming vortex, while in the opposite case σ_2 is dominant), due to rotational symmetry we will need only cross sections integrated over angles. We again approximate the influence of the second member of a KT pair by constant force **F**. The cross sections σ_1 and σ_2 can, in principle, depend on four variables: $F=q^2/R$, the angle θ that the dipole moment makes with the direction of **F**, dipole size λ and distance $R_{\min}$ which characterizes the size of the pinning force. The force **F** is roughly constant because $R\gg\lambda$. These angle-integrated cross sections σ_1 and σ_2 as functions of R for fixed λ and as function of λ for fixed R are plotted in Figs. 7(a) and 7(b), respectively.

One observes that, for R and λ which are not very small, σ_1 is much larger. Only for small λ the cross section σ_2 dominates. It leads to an effective depinning and annihilation of pairs with small binding energy (λ close to $R_{\min}$).

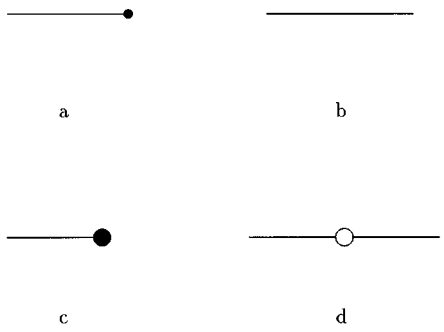

FIG. 8. Elements of the diagrams: (a) Propagation with pinning at some point. (b) Propagation without pinning. (c) Scattering on a pinned dipole at a certain point with resulting destruction of the dipole and pinning of the vortex. (d) Scattering on a pinned dipole at a certain point with resulting destruction of the dipole, but the vortex is not pinned, it continues to move.

VII. THE RG ITERATION: DIAGRAMS AND COMPARISON WITH SIMULATION

Having classified and studied the elementary process involved, we are in a position to convert the iterative process outlined in Sec. V into a recursion equation for $n(R)$, the distribution of surviving KT pairs of size R. To define the RG step, we first divide the vortices at the quenching time into classes. The precise definition is as follows. For a given initial configuration (see Fig. 5) we first find the closest vortex-antivortex pair, then, considering the rest of the vortices only, one find the second closest pair, etc. The process continues until all the vortices and antivortices are distributed as pairs. We define a pair to belong to the ith ''generation'' if the pair's size is between l_i and l_{i+1}. It is natural to define larger intervals for larger pairs. The division is rather arbitrary and we checked that the results are not very sensitive to it.

The distribution of lengths for the overall vortex (and antivortex) density N is given by

$$f(R)=cN^2Re^{-\sqrt{cN}R}, \tag{19}$$

where c is a numerical constant. This was discovered by simulation and probably can be proven mathematically. The normalization is fixed by the requirement that the total density should be equal to N. One can check that $\int_0^\infty f(R)dR=N$. The dimensionless constant is found to be $c\sim 9.5$.

At the beginning of step i one has distribution $n_{i-1}(R)$ of pinned KT pairs from the previous step, density $\rho_i=\rho-2\int_0^\infty n_{i-1}(R)dR$ of the empty pinning centers and distribution $f(R)$ (for $l_i\leqslant R\leqslant l_{i+1}$) of the new KT pairs that start their attempts to annihilate. The difference between the old distribution $n_{i-1}(R)$ and the new one $n_i(R)$ will contain few positive and negative contributions which are convenient to write using diagrams somewhat similar to Feynman diagrams in many-body problems.

One first defines ''propagators.'' There are two kinds of these. The first one [see Fig. 8(a)] is the probability density that a vortex moves past a distance x without encountering any pinning center or pinned pair and then gets pinned around this point. The probability that a particle travels a distance x *and encounters a pinning center in the interval* $(x,x+dx)$ is

$$D_\rho(x)=\rho\sigma e^{-\rho\sigma x}. \tag{20}$$

The second propagator [Fig. 8(b)] denotes the probability that a particle travels a distance x without encountering a pinning center. It is just an exponent:

$$\widetilde{D}_\rho(x)=e^{-\rho_p\sigma x}. \tag{21}$$

Note that while $D_\rho(x)$ has a dimension of 1/cm, $\widetilde{D}_\rho(x)$ is dimensionless.

The σ_1 type and the σ_2 type interactions of a vortex with pinned dipoles can be graphically represented also by Figs. 8(c) and 8(d), respectively. The corresponding expressions are

$$V_1=\int_{R_{\min}}^\infty d\lambda\,\sigma_1(\lambda,R)n(\lambda) \tag{22}$$

and

$$V_1=\int_{R_{\min}}^\infty d\lambda\,\sigma_2(\lambda,R)n(\lambda). \tag{23}$$

Here we integrate over all possible pinned dipole sizes, λ, and $n(\lambda)$ is the current distribution of these sizes. Note also that the cross sections depend on R (which is the distance of the moving dipole to its distant companion). So using Feynmann diagrams language the vertex has many ''flavors'' λ and is nonlocal. Diagrams represent nonintersecting classes of events in a systematic way.

As a simplest example, neglecting the interactions with previously pinned pairs, the survival probability of Sec. IV corresponds only to diagram Fig. 9(a) (also this is the only contribution at the first stage of RG, since no pinned dipoles were considered in Sec. IV):

$$n_0(r)=\int_r^{l_1}dRf(R)\left\{\int_0^{R-r}dx[D_\rho(x)D_\rho(R-r-x)]\right\}, \tag{24}$$

for $r>R_{\min}$. The expression in the curly brackets, after the x integration is performed, coincides with the survival kernel $p(R,r)$ found in Sec. IV without diagrams. Note that propagators depend on the density of unoccupied pinning centers and therefore should be ''updated'' at each RG step:

$$\rho_i=\rho_{i-1}-2\int_{R_{\min}}^\infty n_{i-1}(r)dr. \tag{25}$$

Note also that the density of free pinning centers ρ_i enters the expression *only* via propagators $D_\rho(x)$. Since scattering off pinned dipoles is a rather rare event, it is reasonable to expand in σ_1 and σ_2. All the interactions with empty pinning centers are however summed up to all orders in σ. This is the origin of the exponentials in the propagators. In this paper we limit ourselves to the first order in σ_1 and σ_2 only. The complete list of diagrams is given in Fig. 9. Now we turn to a description of these processes and the explicit details for various contributions.

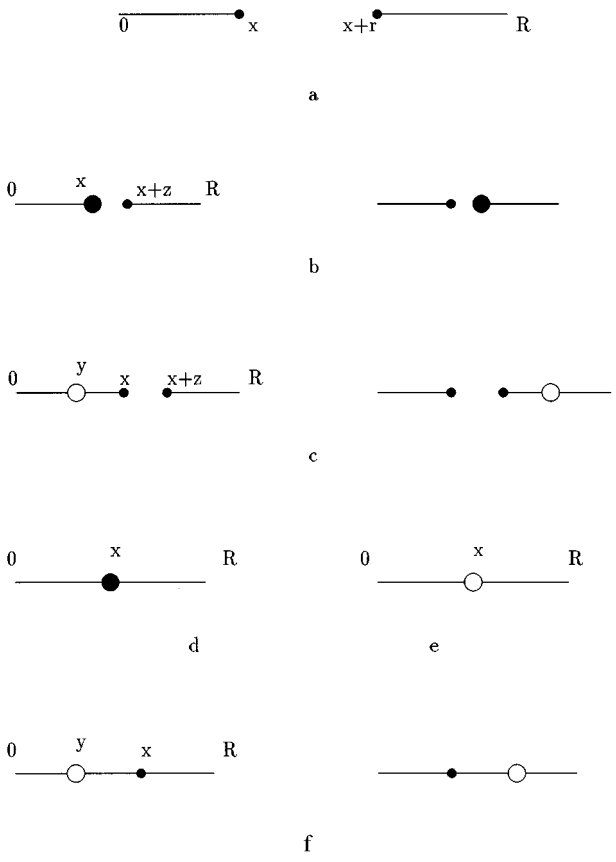

FIG. 9. Diagrams for the RG step (x, y, z and R denote coordinates): (a) Propagation with pinning at two centers. (b) One interaction of the σ_1 type and pinning on another center. (c) One interaction of the σ_2 type with subsequent pinning of both vortices. (d) Both vortices finally got pinned and annihilated on a site where previously a smaller KT pair was destroyed. (e) A small pair is destroyed via the σ_2 process and vortices annihilate. (f) One interaction of the σ_2 type occurs and the pair is subsequently annihilated on the pinning center.

The expression of the contribution in Fig. 9(a) for arbitrary step i (lowest order in interaction with pinned pairs) is just the contribution studied in Secs. II–V. It is positive, in a sense that it always adds pinned pairs. In terms of propagators with updated pinning densities it reads

$$\Delta_i^a(r)=\int_{l_{i-1}}^{l_i} dR f(R)\int_0^{R-r} dx D_{\rho_{i-1}}(x)D_{\rho_{i-1}}(R-r-x)\times\theta(R-r). \tag{26}$$

The interaction with dipoles described by the cross section σ_1, Fig. 9(b) with subsequent pinning of both vortices on different pinning centers adds both positive and negative contributions to the survivors distribution. The positive one: the incoming vortex gets pinned itself by some other pinning center at distance r. We sum over all possible dipole sizes z. Another one is negative: while the interactions might not always cause a pinning, as in (c), it does always cause destruction of the dipole, and we focus on those of size r, summing over all possible final distances z of incoming pairs. Note that the range of integration of z starts from 0 instead of $R_{\min}$, which means that the case when the incoming vortex fails to survive is taken into account [those end up with $z\in(R_{\min},R)$ survive, while those with $z\in(0,R_{\min})$ fail to survive]:

$$\Delta_i^{(b)}=2\int_{l_{i-1}}^{l_i} dR f(R)\int_{R_{\min}}^{R} dz\int_0^{R-z} dx\int_{R_{\min}}^{l_{i-1}} d\lambda \tilde{D}_{\rho_{i-1}}(x)\times(\sigma_1(\lambda,R)n(\lambda))[\delta(z-r)\theta(R-r)-\delta(\lambda-r)]\times D_{\rho_{i-1}}(R-z-x). \tag{27}$$

The σ_2 part of the correction is constructed in a similar manner [Figs. 8(c)]. It is of higher order in pinning density than the σ_1 part:

$$\Delta_i^{(c)}(r)=\int_{l_{i-1}}^{l_i} dR f(R)\int_{R_{\min}}^{R} dz\int_0^{R-z} dx\int_0^{R-z} dy\times\int_{R_{\min}}^{l_{i-1}} d\lambda D_{\rho_{i-1}}(x)(\sigma_2(\lambda,R)n(\lambda))\times[\delta(z-r)\theta(R-r)-\delta(\lambda-r)]D_{\rho_{i-1}}(R-z-x). \tag{28}$$

The other three types of diagrams, Figs. 8(d)–8(f), are simpler and are purely negative. They account for destruction of small KT pairs by vortices of the larger ones which pass by. Subsequently the large pair annihilates by one of three mechanisms:

$$\Delta_i^{(d)}(r)=-\int_{l_{i-1}}^{l_i} dR f(R)\int_0^{R-R_{\min}} dx\int_{R_{\min}}^{l_{i-1}} d\lambda\tilde{D}_{\rho_{i-1}}(x)(\sigma_1(\lambda,R)n(\lambda))\delta(\lambda-r)\tilde{D}_{\rho_{i-1}}(R-R_{\min}-x), \tag{29}$$

$$\Delta_i^{(e)}(r)=-\int_{l_{i-1}}^{l_i} dR f(R)\int_0^{R} dx\int_{R_{\min}}^{l_{i-1}} d\lambda(\sigma_2(\lambda,R)n(\lambda))\delta(\lambda-r)\tilde{D}_{\rho_{i-1}}(R-R_{\min}), \tag{30}$$

$$\Delta_i^{(f)}(r)=-2\int_{l_{i-1}}^{l_i} dR f(R)\int_0^{R-R_{\min}} dy\int_{R_{\min}}^{l_{i-1}} d\lambda\int_y^{R-R_{\min}} dx D_{\rho_{i-1}}(x)(\sigma_2(\lambda,R)n(\lambda))\delta(\lambda-r)\tilde{D}_{\rho_{i-1}}(R-R_{\min}-x). \tag{31}$$

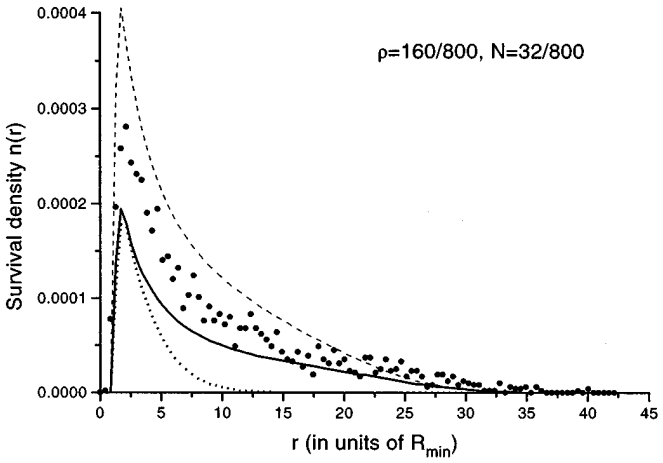

FIG. 10. Distribution of surviving KT pairs. Relatively small pinning density $\rho=0.2\ R_{\min}^{-2}$ and relatively large pair density $N=0.04\ R_{\min}^{-2}$. The dotted line is the infinite sample RG result, the dashed line is the leading-order finite-size RG, while the solid line includes next-to-leading-order corrections.

At the first order in σ_1 and σ_2 the diagram (a) should be modified to take into account the possibility that, in addition to avoiding pinning on centers, the vortex should avoid pinning on dipoles. So there is an additional factor $e^{-\int d\lambda(\sigma_1 n+\sigma_2 n)}\approx 1-\int d\lambda(\sigma_1 n+\sigma_2 n)$. But this contribution precisely cancels with the positive parts of diagrams (b) and (c). Therefore we arrive at the conclusion that the interaction with vortices at first order gives negative contribution (destroys pinned dipole pairs).

All these contributions (diagrams) add up to give the density of dipoles at the beginning of the next step:

$$n_i(r)=n_{i-1}(r)+\sum_{\text{all the diagrams}}\Delta_i(r). \tag{32}$$

Factors of 2 reflect the fact that some diagrams are symmetric with regard to vortex-antivortex exchange. It is assumed that the interaction with pinned dipole corrections are reasonably small. If this is not the case, probability conservation would be violated and one would have to sum up all the orders in σ_1 and σ_2. As we will see, the practical situations do not require this.

We performed up to 60 such iterations steps numerically (so that sizes up to $30R_{\min}$ are covered) and compared the result with direct numerical simulation of the system of size $28R_{\min}\times 28R_{\min}$. The cross sections σ_1 and σ_2 were approximated by the following fit. For $R>\lambda>2R_{\min}$ we use the asymptotic form

$$\sigma_1(\lambda,R)=2.3\sqrt{\lambda R},$$

while for $\lambda_0<\lambda<2R_{\min}$ we use

$$\sigma_1(\lambda,R)=5.05R_{\min}(R/R_{\min}-1)^{0.35}\sqrt{\lambda/R_{\min}-\lambda_0/R_{\min}},$$

which gives correct asymptotics for small λ. Here $\lambda_0\equiv[R/(R-1)]R_{\min}$ is the lower bound for λ, beyond which σ_1 vanishes and σ_2 dominates. The cross section σ_2 can be fitted in all regions that we are interested in by

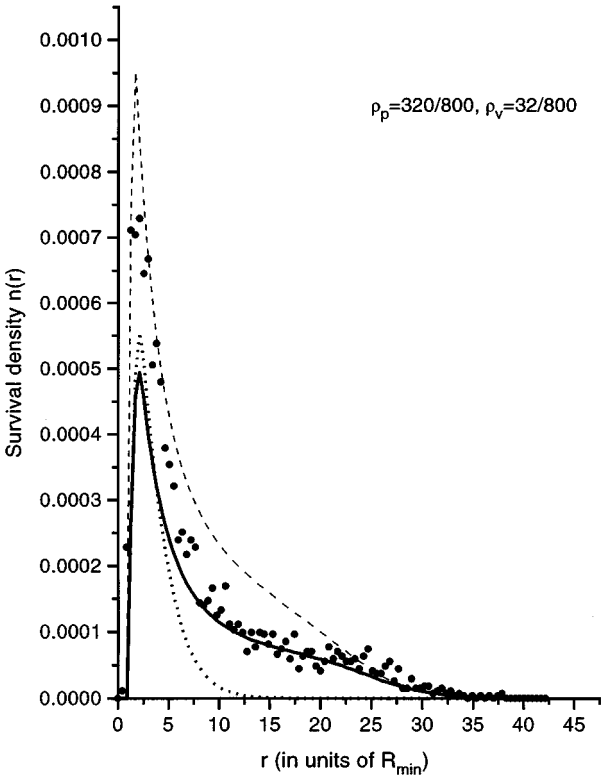

FIG. 11. Distribution of surviving KT pairs. Larger pinning density. $\rho=0.4\ R_{\min}^{-2}$ and relatively large pairs density $N=0.04\ R_{\min}^{-2}$. Same notations as in Fig. 10.

$$\sigma_2=0.59R_{\min}e^{-0.59R/R_{\min}-6.7\lambda/R_{\min}+17}.$$

The results are presented in Figs. 10 and 11 for small and large pinning densities and quite large vortex pair density. The dotted line is the first-order RG result, for the infinite sample. Direct comparison with the simulation results for relatively large r is impossible however, since finite-size effects are still important for the sample size we used. In the next section we show that the RG method can be easily adapted to take into account these effects. This enables us to claim that, despite the fact that we have not established the agreement of the RG calculation in the continuum limit (this requires a surprisingly large lattice and is impossible at this point, as we discuss next), we believe the RG scheme gives reliable results for large samples.

Here we make few comments on the importance of different terms in the RG formula. The interaction with dipole corrections seem to be unimportant in most cases except those at small distances. At small distances, σ_2 is very large due to the instability of small dipoles and the major effect is therefore the destruction of small pairs. On the other hand, σ_1 is important only for large pairs. Further, as the initial density of pairs N gets larger, the peak of $f(R)$ shifts towards smaller R, thus a larger fraction of pairs is inside the $R_{\min}$ region from the beginning. This reduces the total survival probability.

VIII. NUMERICAL SIMULATION: THE EFFECT OF BOUNDARIES

For low pinning density, $\rho=0.2\ R_{\min}^{-2}$ (see Fig. 10) the RG results and numerical simulation results agree very well even

for the vortex pair density as large as $N=0.04\ R_{\min}^{-2}$. The other simulation parameters are: the pinning center's size is $a=0.2\ R_{\min}$. The location of pinning centers as well as of the vortices is randomly generated (a sample contains 10^4 configurations). We tried various boundary conditions. An attempt to employ periodic boundary conditions ran into a problem. We found that for large vortex density the system tends to reach some stable configuration with some vortices (usually one of them) not sitting on any pinning center, while all the others do. In these cases we do not know how to deal with it. If there are no pinnings, this will not happen because of instability to annihilation. This is the case for small vortex density, but for large vortex density it dominates, and there is simply no way to get reasonable data from it. We therefore used a confining boundary condition with a confining potential introduced at the boundary.

To describe the finite-size effects we still can use the iterative scheme, but the distribution $f(R)$ changes considerably for small samples. In addition to the exponentially decreasing ''bulk'' contribution there appears a very slowly decreasing ''boundary'' contribution $f\approx(\sqrt{\rho}/L)R^{-1}$, where L is size of the sample. In our samples, $L=28R_{\min}$, they account for half of the survivors. Performing the finite sample RG we get results denoted by the solid lines in Figs. 10 and 11.

Furthermore, we have neglected the curvature of trajectories (see Fig. 5). In principle the curving of paths should be considered either by using an effective pinning density or by an effective propagator. Large bending is possible when a pair nearby is annihilated. It may not be true that most of the ''initial pairs'' as defined before are still well defined at the final stage of running.

Numerically, take the situation in Y-Ba-Cu-O (Ref. 9) considered before, take $\xi\approx30$ Å, $R_m\approx5\xi=150$ Å, and $\rho\approx600\ \mu\mathrm{m}^{-2}\approx0.1\ R_m^{-2}$. We estimate the vortex density N using Eq. (4), $D^2=(\xi^2/2\pi z)(2T_{\mathrm{KT}}/T-1)$, where D is the mean distance between pairs at temperature T as mentioned before. For $T=T_{\mathrm{KT}}/2$, $D^2=3\xi^2/2\pi z\approx R_m^2/50z$. If $z\approx0.1$, we have $D^2\approx R_m^2/5$ and $N=1/D^2\approx5R_m^{-2}$, this is too large compared to the pinning density and we expect very few pinnings, since essentially most of the pairs are already too close to be pinned. For $z\approx0.01$, we have $D^2\approx2R_m^2$ and $N=1/D^2\approx0.5R_m^{-2}$. By numerical integration we found the total survival density to be roughly $5\times10^{-5}\,R_m^{-2}\approx0.1\ \mu\mathrm{m}^{-2}$. As expected, the survival density in the observable region, i.e., larger than the size of the pickup loop, is small unless the experiment with smaller pickup is feasible. In addition, it is very likely that when the finite-size effect are taken into account properly, the survival probability of the large pairs might be large enough to explain the observed pinnings.

IX. CONCLUSION

In this paper we calculated the probability and size distribution of the KT pair surviving after quenching. By ''quenching'' a reduction of temperature has been meant. There are two qualitatively different cases. The case of rare KT pairs which do not interfere with each other. This case is simple enough to be treated analytically after the basic process of a single vortex attracted to a pinning center in a field of antivortex is studied. A more complicated case is when vortices and antivortices are dense and for a plasma. This case is complicated due to multivortex processes and a more complicated renormalization-group approach should be used. It requires a study of the vortex interacting with an already pinned KT pair.

Now we discuss a practical question of how fast the quenching should be in order that pinned pairs survive. It should be fast enough so that the thermal depinning process will be ineffective to destroy the pairs. It is enough that just one member of the pair is depinned: the pair will very quickly annihilate. The time scale of annihilation of KT pairs without pinning is very short. To be explicit, the time needed for vortex and antivotex separated by R to come to the distance $R_{\min}$ after which they are sure to annihilate is $(R^2-R_{\min}^2)/4\mu q^2$. Taking the mobility in Y-Ba-Cu-O films from Refs. 17 and 18, $\mu=1/(\eta d)\approx5\times10^{13}$ s/kg, where $d\sim3000$ Å is the thickness of the film. Then the annihilation time scale is $\sim10^{-5}$ s for $R=1\ \mu$m.

For thermal depinning to be completely ineffective temperature should be below pinning energy U. Therefore it is very difficult to completely avoid the loss due to thermal depinning. However when one starts at temperatures smaller then U the thermal depinning is not large and cooling can be done rather slowly. Due to pinning, the distribution of KT pairs will not follow adiabatically the equilibrium distribution.

Another way to create vortex-antivortex plasma is to apply external current.[2] This can be done at arbitrarily low temperature. The quenching in this case is just a reduction of the external current. The formulas presented in previous sections apply to this case. One can also consider more complicated situations of ac current, etc. The external magnetic field created additional vortices (organized into Abrikosov lattice or liquid phases[19]). The vortex-antivortex plasma exists alongside these excess vortices. In this situation, however, the annihilation process is greatly accelerated: the antivortex easily finds a vortex to be annihilated.

To conclude, we developed analytical and numerical methods to quantitatively describe the irreversible dynamics of vortex pinnings. The Aharonov-Bohm experiments of direct observation of the KT pair can be understood as a result of simultaneous pinning of both vortex and antivortex. The methods can be applied to a great variety of other situations involving both point pinning and the vortex-antivortex annihilation processes. The surviving Kosterlitz-Thouless pairs can be directly observed using experimental techniques like scanning SQUID microscope. In addition, KT vortices describe any kind of topological defect in 2D, so that dynamical processes studied here occur in great variety of similar systems (vortices in superfluid films, topological defects in 2D lattices, including the Abrikosov vortex lattice in thin films, etc.[3]).

ACKNOWLEDGMENTS

We would like to thank John Chi, Tzay-Ming Hung, Sergei Pozdneev, and Ching-Ping Chen for useful discussions. This work is supported by the National Science Council of Republic of China under Grants No. NSC85-2112-M007-029 and NSC85-2112-M007-032 (for D.C.).

*Electronic address: chang@phys.nthu.edu.tw
†Electronic address: baruch@phys.nthu.edu.tw
‡Electronic address: d833323@phys.nthu.edu.tw

[1] V. Berezinskii Sov. Phys. JETP **34**, 610 (1971); M. Kosterlitz and D. J. Thouless, J. Phys. C **6**, 1181 (1973).

[2] B. I. Halperin and D. R. Nelson, J. Low Temp. Phys. **36**, 599 (1979).

[3] P. Minnhagen, Rev. Mod. Phys. **59**, 213 (1987); Helv. Phys. Acta **65**, 205 (1992).

[4] A. M. Kadin, K. Epstein, and A. M. Goldman, Phys. Rev. B **27**, 6691 (1983); A. T. Fiory, A. F. Hebard, and W. I. Glaberson, *ibid*. **28**, 5075 (1983).

[5] P. C. E. Stamp, L. Forro, and C. Ayache, Phys. Rev. B **38**, 2841 (1988); S. Martin, A. T. Fiory, R. M. Fleming, G. P. Espinosa, and A. S. Cooper, Phys. Rev. Lett. **62**, 677 (1989); N.-C. Yeh and C. C. Tsuei, Phys. Rev. B **39**, 9708 (1989); S. Q. Chen, W. J. Skocpol, E. DeObaldia, M. O'Malley, and P. M. Mankiewich, *ibid*. **47**, 2936 (1993).

[6] J. Pearl, Appl. Phys. Lett. **5**, 65 (1964).

[7] T. Matsuda, A. Fukuhara, T. Yoshida, S. Hasegawa, A. Tonomura, and Q. Ru, Phys. Rev. Lett. **62**, 457 (1991); S. Hasegawa, T. Matsuda, J. Endo, N. Osakabe, M. Igarashi, T. Kobayashi, M. Naito, A. Tonomura, and R. Aoki, Phys. Rev. B **43**, 7631 (1991).

[8] R. C. Black, A. Mathai, F. C. Wellstood, E. Dantsker, A. H. Miklich, D. T. Nemeth, J. J. Kingston, and J. Clarke, Appl. Phys. Lett. **62**, 2128 (1993).

[9] M. J. Ferrari, M. Johnson, F. C. Wellstood, J. J. Kingston, T. J. Shaw, and J. Clarke, J. Low Temp. Phys. **94**, 15 (1994).

[10] L. N. Vu, M. S. Wistrom, and D. J. Van Harlingen, Appl. Phys. Lett. **63**, 1693 (1993); Q. Geng and E. Goto, J. Appl. Phys. **74**, 6293 (1993); J. R. Kirtley *et al.*, Appl. Phys. Lett. **66**, 1138 (1995); Phys. Rev. Lett. **76**, 1336 (1996).

[11] In addition, both pinned particles should survive possible annihilation or depinning by other vortices. This effect is important for stages when the number of vortices is large, in particular in the presence of a magnetic field. We will discuss it later.

[12] J. E. Mooij, in *15th NATO School of Physics* (World Scientific, New York, 1974).

[13] H. Ullmaier, *Irreversible Properties of Type II Superconductors* (Springer-Verlag, New York, 1975).

[14] V. D. Ashkenazy, G. Jung, and B. Ya. Shapiro, Phys. Rev. B **51**, 9118 (1995).

[15] The magnus force, $\eta' \mathbf{n} \times \mathbf{v}$, was estimated to be $\eta' \simeq h n_s/2$ [P. Nozieres and W. F. Vinen, Philos Mag. **14**, 667 (1996)], which can be comparable in size to η in high-T_c materials at low (liquid-helium) temperature. However, in dirty superconductors, this force may be reduced by another force due to impurity interaction [N. B. Kopnin and V. E. Kravtsov, JETP Lett. **23**, 578 (1976); N. B. Kopnin and A. V. Lopatin, Phys. Rev. B **51**, 15 291 (1995)]. For traditional low-T_c superconductors, the Magnus force is known to be negligible while, for high-T_c, the situation is still not so clear experimentally and theoretically [see E. B. Sonin (unpublished) for a recent review]. In this work, we take the simplifying assumption of ignoring the Magnus force. It is possible that, however, it is a lot more complicated to take the Magnus force also into account. The work in that direction is in progress.

[16] V. Ambegaokar, B. I. Halperin, D. R. Nelson, and E. Siggia, Phys. Rev. B **21**, 1806 (1980).

[17] B. A. Willemsen, S. Sridhar, J. S. Derov, and J. H. Silva, Appl. Phys. Lett. **67**, 551 (1995).

[18] S. T. Stoddart, S. J. Bending, A. K. Geim, and M. Henini, Phys. Rev. Lett. **71**, 3854 (1993).

[19] M. E. Fisher, Phys. Rev. B **31**, 2118 (1980).